UM-P-79/38

THE MELBOURNE PROTON MICROPROBE

by G.J.F. LEGGE, C.D. MCKENZIE *and* A.P. MAZZOLINI

School of Physics, University of Melbourne, Parkville, Vic., 3052 AUSTRALIA

Proofs should be sent to:

Dr. G.J.F. Legge
School of Physics,
University of Melbourne,
Parkville, Vic., 3052
AUSTRALIA

Running Title: *Melbourne proton microprobe*

SUMMARY

A scanning proton microprobe is described which operates in ultra-high vacuum with a resolution of ten microns. The operating principles and main features of the design are dis ussed and the ability of such an instrument to detec trace elements down to a few ppm by mass is illustrated.

INTRODUCTION

Recent years have seen the development of several new instruments and techniques for elemental microanalysis. These often provide complementary information, because of the different nature or origin of their strengths and limitations. One of the most promising developments was that of the proton microprobe by Cookson *et al* (1972). In this instrument, the beam of protons or other charged particles from a nuclear accelerator is focussed on to a small aperture. The small beam emerging from this aperture is focussed by a strong magnetic lens to form a demagnified image of the aperture at the surface to be examined. Elemental or isotopic analysis of the specimen is achieved by analysis of the spectra collected by radiation detectors in close proximity to the specimen. The technique is similar in principle to that of the electron microprobe or scanning electron microscope with X-ray attachment. In fact the proton microprobe can also be operated in scanning mode. The most significant characteristics of this instrument are that it is generally non-destructive, it has a mass sensitivity for most elements approaching 1 part per million (1 ppm) when using proton induced X-ray emission (PIXE), and nuclear scattering and reactions may also be used to detect elements or isotopes. The spatial resolution of the proton microprobe is measured in microns and does not yet approach that of a good electron microprobe; however, because of its sensitivity, it is a very powerful tool for trace element microanalysis and is likely to see rapid further development. The Melbourne Proton Micro Probe (MP) is similar in principle to that of Cookson *et al* but differs in many important features. It has now been in operation for two years in its present form but, as will be described below, the basic design allows for further developments.

PROTON SOURCE

The probability of energy exchange between an incoming ion and an atomic electron is generally a maximum when the ion has a velocity which approximates the orbital electron velocity. If the ion itself is an electron, then the above velocity corresponds to the critical energy or ionization threshold; the maximum cross section for ionization and X-ray emission then occurs at a somewhat higher velocity. The K shell ionization energies for elements Na to Zn in the periodic table fall in the range 1 to 10 keV and heavier elements have L or M shell ionization energies within this range. Ignoring other considerations, such as penetration and spatial resolution, we might therefore expect the normal operating range for electron induced X-ray emission (EIXE) to be somewhat higher than the above range of energies. If we now apply similar arguments to the proton, whose mass is about 2000 times that of the electron, we will predict, for maximum PIXE cross section, a beam energy range of about 2 to 20 MeV. However, the ionization thresholds remain in the keV region and background considerations favour beam energies less than the above high values. Consequently, for detection of a wide range of elements, the optimum energy for PIXE is in the vicinity of 3 MeV. This is still an energy which requires the use of a nuclear accelerator. The 5U Pelletron accelerator (National Electrostatics Corporation, Middleton, Wisconsin) at Melbourne is well suited to such a purpose, providing a stable source of protons whose energy is selectable between 0.2 and 5 MeV. The beam optics are good for a nuclear accelerator and relatively large currents can be utilized.

VACUUM SYSTEM

The Pelletron accelerator operates with ultra-high vacuum (UHV) and components of stainless steel, titanium and ceramic. Metal vacuum seals are used. Hydrocarbons (rubbers, plastics, and greases) and high vapour pressure metals are excluded from the system and turbomolecular pumping is employed. This level of vacuum technology has been maintained for MP, which employs an ion pump to attain a pressure of 10^{-9} Torr. The requirements of UHV are

restrictive when movement of some component within the vacuum system must be controlled, stainless steel bellows being in frequent demand. However the ultra-clean conditions maintained are ideal for trace elemental analysis. Naturally any biological specimens must be well dried before they are introduced into such a system. The beam currents employed are generally insufficient to cause problems with outgassing or vaporization of the specimen.

BASIC DESIGN PRINCIPLES

A schematic diagram of MP is shown in Fig. 1. The total length from primary aperture to specimen chamber is 8.7m. The line between the primary aperture and the specimen or beam spot must lie along the magnetic axis of the probe-forming lens and the three components - primary aperture, magnetic lens and specimen mount - must maintain this condition to high precision over a long period. The diaphragm which limits the aperture, and hence the aberrations of the lens, should also be stably positioned on the above line. The above considerations will affect the position and spatial resolution (probe spot size) of the beam. It is also necessary that the above line or axis of MP be readily aligned with the axis of the beam emerging from the Pelletron accelerator. If spatial resolution is set by the diaphragm, then relative misalignment of these two axes will simply lead to a reduction in available beam current. To cope with these problems, all components of MP have been mounted on a 360mm square 6 mm thick horizontal steel box girder of 8.6m length. This can be seen in the photograph of Fig. 2. The primary or entrance aperture, iris diaphragm, lenses and specimen support are mounted directly on the box girder. The primary aperture, iris diaphragm and specimen support are mechanically isolated from the beam line and specimen chamber by means of stainless steel bellows. In each case there are two bellows mounted in opposition so as to balance out all vacuum forces. It is thus possible to let up and pump down the vacuum system or to knock the beam line or specimen chamber without fear of moving the specimen or upsetting the alignment.

The box girder itself is supported on two steel pedestals, one directly beneath the primary aperture and one at the other end of the girder beneath the lens. Each support provides three-dimensional adjustment of position. Thus, once the beam from the accelerator has been centred on the primary aperture, the girder may be pivoted about the aperture until the optical axis of MP coincides with the accelerator beam axis.

MONITOR CUP

The exit or energy analysing slit of the Pelletron accelerator is normally set at a gap of 1 mm and the beam focus at this point is of comparable dimensions. The accelerator can deliver through this slit into MP a proton current of up to 5×10^{-5} A at an energy of 3 MeV. Of this 150 Watt, spread over a 1 mm diameter area, only the inner core of beam will be used and, in the interests of geometrical stability, this much power should not be dumped on the primary aperture. Most of the beam therefore is collected with a Faraday cup in front of the primary aperture. This cup, made of molybdenum, is clamped by two beryllium oxide insulating washers onto a water-cooled copper block and has a central hole of 500 μm diameter in its tantalum backplate. Thus about 75% of the accelerator beam is collected by the cup, which thereby provides a continuous monitor of the beam current supplied by the accelerator.

PRIMARY APERTURE

The primary aperture design is important to the size, stability and sharpness of the microprobe focal spot. Versatility is obviously achieved by the use of a double slit, which enables rectangular focal spots to be produced with maximum available beam. However, if needed, such a spot shape can be produced from a circular aperture by defocussing with the lens or by scanning the beam. The principle objections to slits stem from the mechanical instability, non reproducability, uncertainty and replacement difficulties which can occur. In order to maintain geometrical stability, the aperture should be water cooled and it should be readily removable for inspection or replacement, with automatic

precise realignment, all of which is much easier to achieve with a simple aperture. The steady accumulation of carbon which arises from cracked hydrocarbons is a problem in many accelerators and electron microprobes, and such deposition can readily block a small aperture; carbon can also deposit on slit surfaces and produce rough edges or non-closing slits. Some electron microscopes avoid this problem by ensuring that apertures are maintained at a high temperature by beam bombardment and poor cooling. In MP, however, this is unnecessary because of the low hydro-carbon level which is maintained. The primary aperture is selected from a line of apertures in a tantalum plate supplied by JEOL as a standard objective aperture strip for electron microscopes. The aperture strip is clamped in a stainless steel wedge (Fig. 3) against a copper block. The wedge is readily removeable for inspection or replacement. When slid into place, the wedge, and hence the aperture strip, is automatically realigned and the copper block is pressed against a water cooled surface. This system has now given trouble-free use for over two years with no sign of deposition on the apertures and only slight wear. The various diameter apertures (20, 40, 60, 120 μm) are selected by a sideways movement of the entire structure to a positional accuracy of 1 μm.

Scattering of protons from the edges of the aperture must be minimized if a well defined focussed spot is required at the specimen. With thick slits this can be achieved (Nobiling *et al*, 1975) by careful shaping of the slit edges. With MP it has been achieved by the use of a thin aperture plate and a small (1 mrad.) angular convergence of the beam at the aperture. Ideally, for this method of scattering suppression, the thickness of the aperture plate should just exceed the range of the protons. For 3 MeV protons in tantalum this is 32 μm. However, even with a slightly thinner aperture plate, a sharply focussed beam spot was achieved, because protons which traversed the plate around the aperture emerged with very low energy and a wide angular spread due to multiple scattering through the plate. Very few of these low energy protons could navigate both the following iris diaphragm and the strong magnetic lenses. Even those that did would be very inefficient in X-ray production and hence insignificant.

IRIS DIAPHRAGM

Aberrations of the lens are controlled by placement of an iris diaphragm 5 m after the primary aperture. This diaphragm can be axially positioned to an accuracy of about 100 μm. It is made from a standard camera iris diaphragm, the steel leaves of the iris being replaced by thin tantalum leaves. The range of openings available is 2mm to 15mm. Position and opening are controlled from outside the vacuum line. No water cooling is needed on this diaphragm because the beam here is attenuated and unfocussed.

PROBE FORMING LENS

A 3 MeV beam of protons is too magnetically rigid to be usefully focussed by an axially symmetric iron lens of the type used in electron instruments. It is necessary to use strong focussing as provided by a magnetic quadrupole. At least two such quadrupole lenses are needed to produce overall focussing of all rays, since a single quadrupole lens will focus in one plane and defocus in the perpendicular plane. Following Cookson *et al*, we have used four quadrupole lenses in a configuration known as a *Russian quadruplet* because of the thorough investigations into such a system by Dymnikov *et al* (1965). Such an antisymmetric system, in which the lenses alternate in polarity, the first and fourth lenses being of equal strength and likewise the second and third lenses, results in orthomorphic stigmatic focussing. We chose to utilize some old magnetic quadrupole lenses (Lintott Engineering, Horsham, Sussex) which were available from the beam line of a decommissioned accelerator. These lenses, each 120 mm in length of pole, were not designed for such precision focussing as that of a microprobe; but measurement showed the 50 mm bores to be uniform to 10 μm and the interpole gaps of 19 mm were uniform to 70 μm. The coils were also found to be well matched. Magnetic centres were located for each lens, by the polarization method of Cobb and Muray (1967), and found to lie within 100 μm of the geometric centres. This was about the accuracy of the measurement; so, to a first approximation, the magnetic and geometrical centres were assumed to

coincide. Because the microprobe line was to be in part a test facility, rather than a final design, and because it is useful to be able to change the focal length of the lens system without moving the specimen chamber, the four lenses were mounted on separate trolleys on a 25 mm thick steel bed and 25 mm diameter rail of 3 m length. The table and rail were levelled to an overall accuracy of 10 μm. The rail was optically aligned to be parallel to the axis of the beam, as defined by the primary aperture, the iris diaphragm and the geometrical centres of the lenses, to an accuracy of 10 μm. It was then possible to move a lens the length of the baseplate and to keep it on axis within 10 μm. Each trolley carried adjustments for horizontal and vertical alignment of its lens and for rotation about the optical axis. Rotation about a vertical axis was possible but not needed. As shown by Crewe *et al* (1967) for electron lenses and by Cookson *et al* (1972) for proton lenses, the only important rotational adjustment is that about the optical axis and this adjustement is a critical one. Final alignment was done with the proton beam by elimination of steering effects for each individual lens in turn, in both focussing planes. Rotational alignment was obtained by seeking an optimum focus - minimum probe spot diameter.

The lens currents were obtained from model 246A current supplies (BWD Electronics, Mulgrave, Vic., Australia). The specifications on these units are only 1000 ppm current stability and an effective 100 ppm ripple. However they may be wired for external control with fast response. It was therefore possible to add an external controller incorporating a high stability reference voltage, decapots (Electro Scientific Industries, Portland, Oregon), voltage comparators and standard resistors to measure the lens currents. The controller with its four decapots is seen in the foreground of Fig. 2. The modified supplies then gave a current stability of 5 ppm (1 ppm short term). The ripple was likewise brought down to a level of 10 ppm RMS, because of the fast response of the circuitry. These figures are more than adequate for the present requirements. Thermal stability was not independently measured, since the laboratory is air conditioned, but it should likewise be determined by the good thermal stabilities of the voltage comparators (LH0052D), reference voltage (IN829A), decapots and

standard resistors, all of which were 5 ppm $(^{\circ}C)^{-1}$ or better.

SPECIMEN CHAMBER

The specimen chamber seen at the left hand end of the beam line in Fig. 2 was designed as the simplest method of obtaining several ports at 45° to the beam axis. It is machined out of a solid cylinder of stainless steel and externally comprises an octagon of standard knife-edge seals. All seals, as elsewhere, are made with copper or gold gaskets, except for seals onto glass, where indium is used. Flanges have 70 mm overall diameter and ports have 35 mm internal diameter. The chamber has an internal diameter of 125 mm. One of the two octagonal faces is sealed with a glass plate providing an unrestricted view (Fig. 4) of the entire chamber. In Fig. 4, the beam enters from the left. The specimen is supported on the central plate from a micrometer stage beneath the chamber and visible in Fig. 2. The coupling is a rigid one through stainless steel bellows. By this means, a specimen may be reliably located to an accuracy of 1 μm. Specimens are inserted through the top port, which also provides the connection to a turbomolecular pump used for roughing down to 10^{-7} Torr. Biological specimens are normally mounted on thin nylon foils made by the method of Brown *et al.* (1948) modified by Hall (1972). These specimens are viewed by a microscope in transmission mode. Illumination is of necessity dark field, with the light source outside the chamber. The apparatus on the right of Fig. 4 enables a Faraday cup to be replaced by either of two objective lenses, mounted in a stainless steel block on either side of the Faraday cup. This block is driven along a smooth V-block by means of a screw thread and a rotary high vacuum feedthrough, visible in Fig. 2 on the right of the chamber. The binocular eyepiece for the microscope is mounted outside the chamber directly onto a glass viewport. Overall magnifications available are X200 or X400. Solid specimens are viewed from the front by means of an internal mirror and an external stereo zoom microscope, neither of which are shown in Fig. 4. The maximum magnification obtained with this front viewing microscope is X60.

Figure 4 also shows the snout of a Si(Li) X-ray detector at 45° above the beam axis on the left. [illegible] thick beryllium foil is clipped over the snout to keep out backscattered protons. This detector was specially made (Ortec Inc., Oak Ridge, Tennessee) with a knife-edge seal. It is retractable through a stainless steel bellows as the dewar is raised up a 45° ramp seen in Fig. 2. The Si(Li) crystal gives an energy resolution of 155 eV at 6 keV, has an area of 12.5 mm^2 and can be brought within 20 mm of the specimen. Below the beam axis on the left of Fig. 4 is a surface barrier detector to measure the energy spectrum of back scattered protons. A similar detector can be mounted in the holder above the Faraday cup on the right and at 45° to the beam axis. This detector measures the energy spectrum of forward scattered protons from a thin specimen. If nuclear reactions are to be utilized, for isotopic analysis of the specimens, the above surface barrier detectors may be used to detect charged particles and neutron or gamma ray detectors may be mounted outside the chamber.

DEFLECTION SYSTEM

The proton beam can be deflected in any direction by up to 1 mm at the specimen by means of two saddle coils. These are wound according to the method of Dressel and Soller (1948) to give a uniform field and are placed ahead of the lens in order to leave as much clearance as possible for radiation detectors to be placed between the lens and the specimen. The decision to use magnetic, rather than electrostatic, deflection was based on the greater degree of freedom then obtained in positioning of the coils anywhere along the beam tubing, on the greater space then available to produce a uniform field and on the ultimate requirement that fast linear scanning be available. The latter requirement implied high power scanning circuitry which seemed simpler to obtain with high currents than with high voltages. It also dictated the use of iron free coils. The coils are powered by two waveform and offset generators driving current amplifiers. Deflection currents are measured directly by means of series resistors in the current leads, so that any non linearities in the electronics

will not produce distortion in tracking of the beam spot or imaging of a specimen, though they will of course still change the beam deflection from its intended value and may thus give rise to non uniform coverage of a specimen. Although the present placement of the deflection coils ahead of the lens magnets is satisfactory for the present resolution and for beam deflections limited to 1 mm, it remains to be seen whether the off-axis aberrations so produced become significant when the present lenses are replaced in a quest for better resolution.

We have followed Cookson *et al* in using triangular waveforms for both X and Y scans, rather than the usual sawtooth waveforms. This avoids the necessity of gating off electronics during flyback of the beam. However, if fast scanning rates are used, it is essential that any electronic delays be compensated for; otherwise double or quadruple imaging of a specimen will obviously result. The scanning frequencies are variable but selected to be comparable so that any heating of the specimen by the beam is as uniform as possible. It is of course necessary then to ensure that the two frequencies selected do not produce a closed Lissajous figure, but cause the probe to cover the specimen in a uniform manner. The incidence of a proton on the specimen may be accompanied by the emission of some form of radiation, the energy of which is characteristic of the emitting atom. The signals from a radiation detector at the specimen may be utilized together with the X and Y deflection signals to produce a map of all emitting locations on the screen of a storage oscilloscope and such a system is used to set up specimens. In a manner familiar to users of scanning electron microprobes, a single channel analyser could be used to select a chosen range of energies and hence to produce a map of a chosen elemental distribution. However the system of scanning analysis developed on MP is more comprehensive than this and will be described in a subsequent paper (Legge and Hammond, 1979).

PERFORMANCE

The important characteristics of a microprobe are the spatial resolution, as determined by the diameter of the focussed beam spot, and the sensitivity, as determined by the level of any background radiation.

Spatial Resolution

The beam spot diameter obviously depends on the aperture diameter, the lens demagnification factor and aberrations - of both geometrical and mechanical origin. The geometry of MP, as explained above, is readily adjustable. The present magnets are usually placed in the close geometry shown in Fig. 1. For this geometry, the coil currents for the inner magnets must be approximately twice those for the outer magnets and the demagnification factor of the combination lens is about 1/9. If the primary aperture is repeatedly reduced in size, the focussed spot size will eventually approach a limit set by aberrations; and if the iris diaphragm is then steadily reduced in size, the spherical aberration will steadily diminish until the mechanical aberrations dominate. Nobiling *et al* (1977) report a spot size limit of 2 μm for a precision doublet lens at 2 MeV and beam currents of 2 to 8 × 10^{-11} A. The present quadruplet lens on MP sets a limit of 10 μm spot size with the minimum primary aperture of 20 μm and the minimum iris diaphragm opening of 2 mm. At the usual beam energy of 3 MeV, a current of 3 × 10^{-6} A from the Pelletron accelerator (readily obtained with an exit slit gap of 1 mm) produces a current of 2 × 10^{-9} A through the 20 μm aperture, of which 1 × 10^{-9} A passes through the 2 mm iris diaphragm to reach the specimen in a focussed spot. This is sufficient beam current for most applications but, by increasing the aperture size, more current is available without greatly increasing the spot size. 10 μm is therefore the spatial resolution usually achieved. This is the diameter of the focussed spot observed on a glass plate by means of the rear microscope and spots of the same diameter have been burnt through plastic foils. Further measurements, in which the beam was scanned across a metal edge, have shown that the apparent spot diameter is in fact the width at half height of a radial distribution of beam intensity which is close to Gaussian. This distribution is almost entirely due to mechanical inaccuracies of the present magnets. Since we intend to replace these magnets with precision ones which should give much better resolution, being limited mainly by small geometrical aberrations, there is no point in further comment, except to emphasize the absence of any halo around the present Gaussian distribution.

Sensitivity

The sensitivity of elemental detection provided by electron induced X-ray emission (EIXE) or by proton induced X-ray emission (PIXE) is ultimately limited by the level of any background radiation. This may take the form of continuous or discrete radiation. Such backgrounds can be subtracted off, but their presence can greatly increase the statistical uncertainty in estimating an elemental concentration and, in the case of discrete radiation, the background level may be variable or difficult to determine because it is specimen dependent. The continuous radiation provides a basic limitation, because such a *bremsstrahlung* continuum is inherently associated with the interaction of charged particles with matter. However a proton or other positive ion, being much heavier than an electron, will decelerate and therefore radiate energy at a much lower rate. Consequently, at high X-ray energies, the continuous background from PIXE is much lower than that from EIXE. At low X-ray energies, the difference may not be so marked (depending on the proton energy), but the PIXE background is lower, coming mainly from knock-on electrons or *delta rays* (Folkmann *et al*, 1974). Discrete background radiation often arises in X-ray spectra from electron microprobes because the electrons are readily scattered by the specimen on to neighbouring surfaces and the characteristic radiation from these surfaces can often reach the X-ray detector. The fluorescence radiation produced in the specimen and its surroundings by the X-ray continuum background may also be regarded as a source of discrete background radiation. Again, protons or heavier ions, being less readily deflected and producing little continuum radiation, are less likely to cause such discrete background problems. Likewise, any discrete radiation produced by a microbeam halo could also be regarded effectively as background radiation. It is inadvisable to place any beam collimators in the vicinity of the specimen, because of the halo of scattered beam thus generated. With a high energy beam, gamma rays may also be produced and it is difficult to shield the X-ray detector from such high energy rays which deposit energy by Compton scattering (Folkmann *et al*,

1974). The only collimator on MP is 3.7 m from the X-ray detector and, for thin specimens, the beam is stopped on carbon 55 mm from the detector (only the 1% abundant isotope ^{13}C can be a source of gamma rays for a proton energy of 3 MeV). The limiting elemental mass sensitivity for MP in the important region of the heavy metals has been estimated as 1 ppm in the analysed specimen. However such low levels require large beam charge and the effective sensitivity is best indicated by the examples and comparisons of the following section.

APPLICATIONS

In order to illustrate the performance of MP in spot analysis, we will give examples of PIXE and nuclear scattering spectra measured with thin biological specimens and one application of PIXE to a thick geological sample. For further examples of such techniques we refer the reader to the original paper on the Harwell proton microprobe (Cookson *et al*, 1972) and later papers on solid state specimens (Cookson and Pilling, 1975) and on biological specimens (Cookson and Legge, 1975). The two latter papers include examples of nuclear reactions used for isotopic depth profiling and line scanning, topics not covered in this paper. Further examples and general techniques of Ion Beam Analysis are given in the proceedings of a conference (Wolicki *et al.*, 1978).

Biological Specimens

A biological example of an X-ray spectrum taken with the Si(Li) detector on MP is shown in Fig. 5. The specimen, prepared by Dr. C.K. Pallaghy, was a freeze-dried epidermal strip of wheat leaf supported on a thin nylon foil and the proton beam was focussed on a stoma complex. This represented a fairly thin target to the proton beam which traversed it and was stopped in the Faraday cup. The beam energy was 3 MeV and the beam current was 2.5×10^{-10}A for 9000 sec. The characteristic X-rays detected and identified in the figure all originated in the specimen and are not present in foil or background spectra. In the very low energy region of the spectrum, the light element peaks, representing a few percent of the specimen mass, sit on a continuum of

comparable height. X-rays from the elements lighter than silicon were heavily suppressed by the beryllium window and proton absorber in front of the Si(Li) detector. The X-ray continuum is mostly generated by secondary electrons from the carbon of the specimen matrix. However, in this light element region of the spectrum, the counting statistics are good and the continuum background decreases rapidly with increasing X-ray energy. It is negligible beneath the potassium peak and continues to decrease in the important region of the heavy metals, as shown by the expanded scale regions of Fig. 5. The copper peak in this spectrum represents an elemental abundance in the undried specimen of about 10 ppm by weight and the heaviest elements observed were close to the ppm level. The limitation here is counting statistics rather than background.

The background for PIXE is generally so low that a Si(Li) detector can achieve a sufficiently high peak to background ratio to measure most elemental abundances. There is seldom the necessity to employ a wavelength dispersive detector with its superior resolution and hence higher peak to background ratio but limitation to a single energy channel, although it may be needed to resolve some cases of peak interference. With many biological specimens, a weak calcium Kα line is masked by a strong potassium Kβ line; but in such cases the even weaker calcium Kβ line is usually detectable with a Si(Li) detector, as illustrated in Fig. 5. Specimen damage and elemental loss rate with PIXE is comparable to that occuring with EIXE and it can be similarly related to X-ray production rates. When information on many elements is required from biological specimens, there is a strong argument for collecting all of this information simultaneously with a Si(Li) detector and therefore requiring only a relatively low beam current in order to complete the task in a reasonable time. This argument holds also when elemental distributions are required (Legge and Hammond, 1979) because, although the maximum permissable current is higher when the beam is scanned, the amount of information sought is much greater.

With biological specimens, the very light elements - hydrogen, carbon, nitrogen and oxygen - form the matrix. Nitrogen is indicative of proteins and nucleic acids. The other elements can provide a measure of specimen thickness and of moisture content. With thin specimens, an energy spectrum of forward-

scattered protons will show a well-isolated peak for hydrogen in what is essentially a mass spectrum. Fig. 6 shows the spectrum of protons scattered at 45° from a dessicator-dried single skin fibroblast cell plated on a nylon foil by Dr. G. Hodgson and Dr. R. Bradley. The hydrogen peak is subject to *kinematic broadening* unless the angle of scatter is narrowly defined; however the peak is so isolated that such broadening can be tolerated and, in this case, a detector of large solid angle (0.2 sr.) was used to give a total count of 2×10^5 in the hydrogen peak with a beam current of 2×10^{-10}A for 1000 sec The microbeam energy was 3 MeV. The peak near full energy, with a total count comparable to that of hydrogen, represents mostly protons scattered from carbon, but with significant contributions from the less abundant nitrogen and oxygen of the dried specimen.

For thin specimens (a few microns in thickness), these contributions can be separated at backward scattering angles, providing the range of scattering angles seen by the detector is restricted. For a collimated detector at backward scattering angles the count rate will be relatively low; but it is adequate even for the thin nylon backing foil, whose contribution must be subtracted from that for a supported specimen. Fig. 7. shows such a spectrum of protons scattered from a nylon foil at 135°. The microbeam current was 5×10^{-10}A at 3 MeV for 1000 sec and the carbon peak contains a total count of 4,000. A slit restricted the accepted scattering angles to a range of 0.05 rad. and the solid angle was 0.02 sr.

Geological Specimens

Much of the above discussion concerning biological specimens is also relevant to a discussion concerning nonbiological specimens. The major differences are the generally heavier atomic number of the matrix elements for nonbiological specimens and the greater likelihood that nonbiological specimens will be thick, that is opaque to the proton beam. Both these factors will tend to increase the background radiation level in PIXE analysis with respect to the level of characteristic radiation, but this is generally offset by the ability of specimens to withstand large beam currents and hence to yield good

counting statistics. As with biological specimens, the background is very low in the high energy region of a PIXE spectrum and the proton microprobe is very useful in identifying trace concentrations of *rare earths* and other heavy elements in geological samples.

Figure 8 shows a direct comparison between the X-ray spectra generated by a JEOL scanning electron microscope (SEM) and by MP from the same thick sample of *Xenotime* prepared by Mr. T.C. Hughes. The two Si(Li) detectors involved had very similar resolution. The two spectra have been normalized to show approximately the same peak heights for characteristic radiation and are plotted on the same baseline without any corrections. The continuous background level is notably different for the two microprobes with consequent differences in statistical uncertainties and hence detection limits. The true background for MP is not observable on the scale of Fig. 8. It is below that for the SEM by approximately a factor of 10^3. The exposures were 4×10^{-10}A of 35 keV electrons for 10 min. and 10^{-9}A of 3 MeV protons for 25 min.

ACKNOWLEDGEMENTS

This work was supported in part by the Australian Research Grants Committee and also benefited greatly from the availability of vacuum equipment purchased on an earlier grant from the Nuffield Foundation.

We are grateful to Dr. T.A. Hall for advice on the manufacture of nylon foils and for his assistance in the procurring of suitable materials. We thank Dr. C.K. Pallaghy, Dr. G.S. Hodgson, Dr. R. Bradley and Mr. T.C. Hughes for permission to show spectra obtained from their specimens and we thank Mr. D. Sewell for performing the SEM analysis of *Xenotime*.

Several members of our school have contributed to the development of MP and we would particularly thank Mr. C.S. Papper for the design and contruction of the scanning coils and members of the three workshops for their precision and ccoperation which made this project possible.

We are most indebted to Dr. J.A. Cookson, Mr. F.D. Pilling and Dr. A.T.G. Ferguson for their pioneering work with proton microprobes, and two of us (G.J.F.L. and C.D.McK.) particularly thank them for their hospitality at AERE Harwell and the benefits of their knowledge and experience before this work was commenced.

References

Brown, J., Felber, F., Richards, J. & Saxon, D. (1948) On making thin nylon films. *Rev. Sci. Instrum.* 19, 818.

Cobb, J.K. & Muray, J.J. (1967) Magnetic center location in multipole fields. *Nucl. Instr. and Meth.* 46, 99.

Cookson, J.A., Ferguson, A.T.G. & Pilling, F.D. (1972) Proton microbeams, their production and use. *J. Radioanalyt. Chem.* 12, 39.

Cookson, J.A. & Pilling, F.D. (1973) The use of focussed ion beams for analysis. *Thin Solid Films.* 19, 381.

Cookson, J.A. & Legge, G.J.F. (1975) Biological analysis with a nuclear microprobe. *Proc. Analyt. Div. Chem. Soc.* 12, 225.

Crewe, A.V., Eggenberger, D.N. Welter, L.M. & Wall, J. (1967) Experiments with quadrupole lenses in a scanning microscope. *J. Appl. Phys.* 38, 4257.

Dressel, R. & Soller, T. (1948) Construction and characteristics of deflection coils. In: *Cathode Ray Tube Displays* (Ed. by T. Soller, M.A. Starr & G.E. Valley). p. 712. McGraw-Hill, New York.

Dymnikov, A.D., Fishkova, T. Ya. & Yavor, S. Ya. (1965) Effect of geometrical parameters on optical characteristics of a system of four quadrupole lenses similar to an axisymmetric lens. *Soviet Phys.-Tech. Phys.* 10, 340.

Folkmann, F., Gaarde, C., Huus, T. & Kemp, K. (1974) Proton induced X-ray emission as a tool for trace element analysis. *Nucl. Instr. and Meth.* 116, 487.

Hall, T.A., Röckert, H.O.E. & Saunders, R.L. de C.H. (1972) *X-ray Microscopy in Clinical and Experimental Medicine.* Charles C. Thomas, Springfield Ill.

Legge, G.J.F. & Hammond, I. (1979) Total quantitative recording of elemental maps and spectra with a scanning microprobe. *J. Microsc.*

Nobiling, R., Civelekoglu, Y., Povh, B., Schwalm, D. & Traxel, K. (1975) Collimation of ion beams to micrometer dimensions. *Nucl. Instr. and Meth.* 130, 325.

References (cont'd)

Nobiling, R., Traxel, K., Bosch, F., Civelekoglu, Y., Martin, B. & Povh, B. (1977) Focussing of proton beams to micrometer dimensions. *Nucl. Instr. and Meth.* 142, 49.

Wolicki, E.A., Butler, J.W. & Treado, P.A., ed. (1978). Proc. 3rd Int. Conf. on Ion Beam Analysis. *Nucl. Instr. and Meth.* 149, 1-759.

Fig. 1. Schematic diagram (not to scale) of the proton microprobe (MP) showing the principal components and their relative positions. M: monitor cup with 500 μm hole in backplate; A: principal aperture (20-120 μm); I: iris diaphragm (2-15 mm); L: combination lens (4 magnetic quadrupoles); S: specimen holder; C: Faraday cup (interchangeable with optical microscope objectives); E: binocular eyepiece for optical microscope; O: octagonal specimen chamber; X: X-ray detector (Si(Li)); B: back-scattered proton detector; F: forward-scattered proton detector. The spacings are given in mm.

Fig. 2. Photograph of MP, with the primary aperture at the far right, the 4 magnetic quadrupoles in the centre and the octagonal specimen chamber at the left hand end of the beam line. All are mounted on a steel box girder. The sweep coils can be seen just to the right of the quadrupoles.

Fig. 3. The primary aperture wedge removed from the water-cooled support rod. This support rod, which is positioned by a transverse micrometer screw, carries a double chamfer groove on its front face into which the wedge slides, thereby clamping the aperture strip inside the wedge against the copper block seen above in the back reflection of the wedge. At the same time the copper is clamped against the water cooled surface and the wedge is accurately located.

Fig. 4. Photograph of the specimen chamber interior, showing the beam entry port on the left, the X-ray and back scattered proton detectors above and below this port respectively, the central specimen (supported from a micrometer stage beneath the chamber), a Faraday cup on the right to collect the beam and the mount for a forward scattered proton detector above the Faraday cup. The screw thread beneath the cup enables it to be replaced by either of 2 optical microscope objective lenses.

Fig. 5. X-ray spectrum of a freeze-dried wheat leaf epidermis with the proton beam from MP focussed on a stomatal complex. The specimen was supported on nylon foil, the beam was 2.5×10^{-10}A of 3 MeV protons for 9000 sec. and the detector was a Si(Li) detector. Except for the Pb lines, all radiation was K radiation and, unless labelled β, was Kα radiation. The weak peaks on the right from the heavy elements, which are statistically weak but significant, are close to the ppm level referred to the original specimen wet weight.

Fig. 6. Spectrum of protons scattered at 45° from a dessicator-dried skin fibroblast cell into a surface barrier detector. The cell was mounted on nylon foil; the 3 MeV proton beam from MP focussed on the cell was 2×10^{-10}A for 1000 sec. The wide peak on the left represents protons scattered from hydrogen nuclei in the specimen and the peak on the right is mostly due to carbon.

Fig. 7. Spectrum of protons scattered at 135° from a nylon foil into a surface barrier detector. The 3 MeV proton beam from MP was 5×10^{-10}A for 1000 sec. The three peaks, from left to right, show the contributions from carbon, nitrogen and oxygen in the specimen. Hydrogen is not observed in such a back-scattered spectrum, for kinematic reasons.

Fig. 8. X-ray spectra from a thick specimen of *Xenotime*. The two spectra were measured with Si(Li) detectors of similar energy resolution and have the same baseline, no background having been subtracted from either spectrum. The upper spectrum comes from a JEOL electron microscope and the lower one from MP. The two spectra have been normalized to show similar peak heights, so that the peak-to-background ratios might be compared. The incompletely resolved group of peaks on the left are L radiation from [illegible] elements and the strong peaks on the right are K radiation from yttrium. The exposures were 4×10^{-11}A of 35 keV electrons for 10 min. and 10^{-9}A of 3 MeV protons for 25 min.

Legge, McKenzie & Mazzolini Figure 1

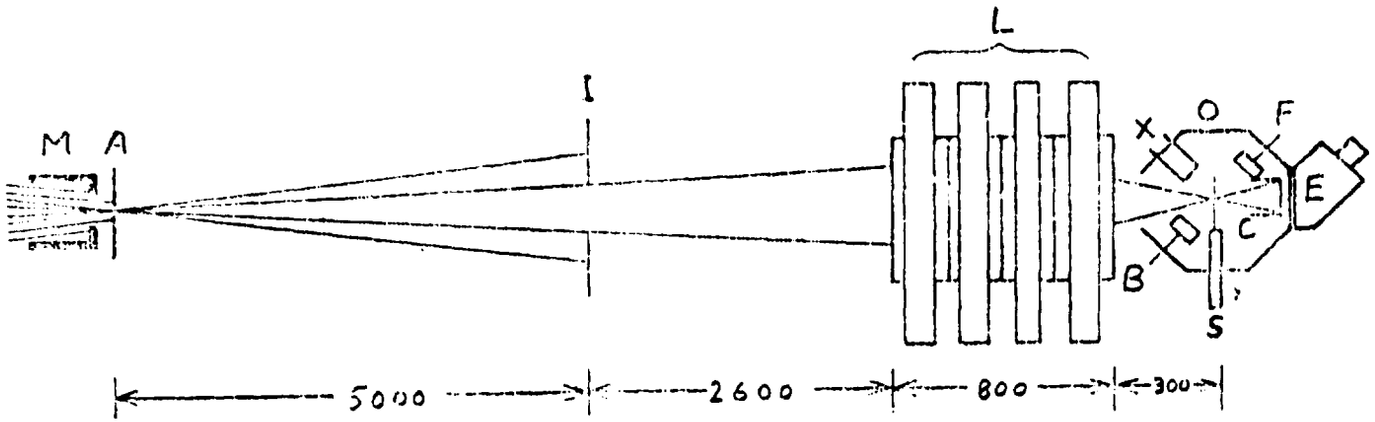

Figure 1

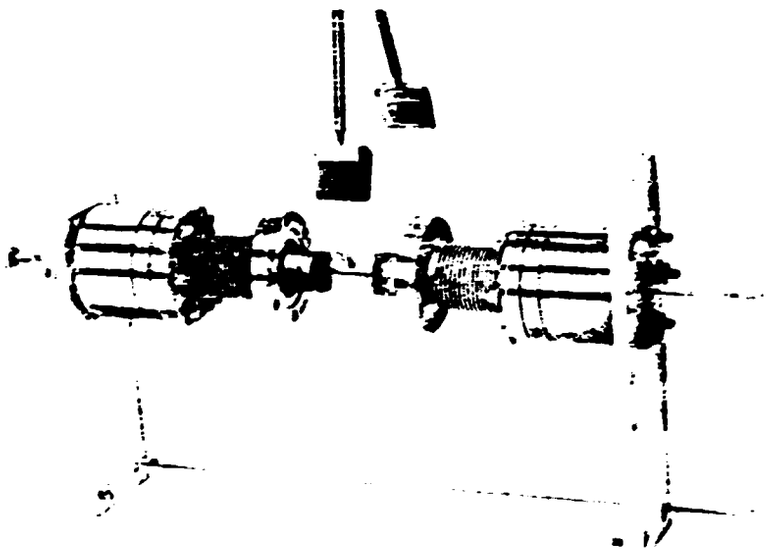

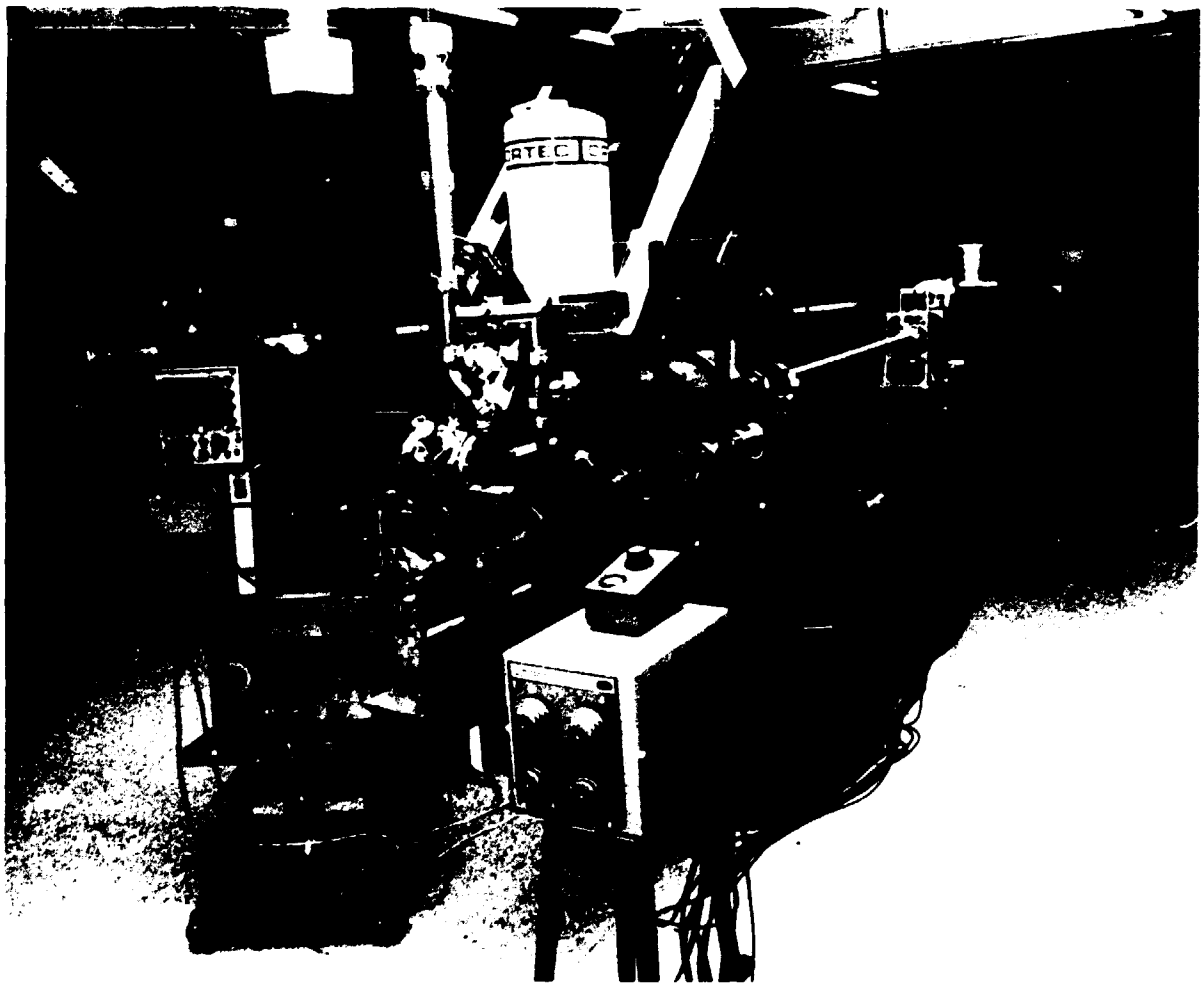

Fig. 2: MP

Fig. 4 : MP
Specimen chamber

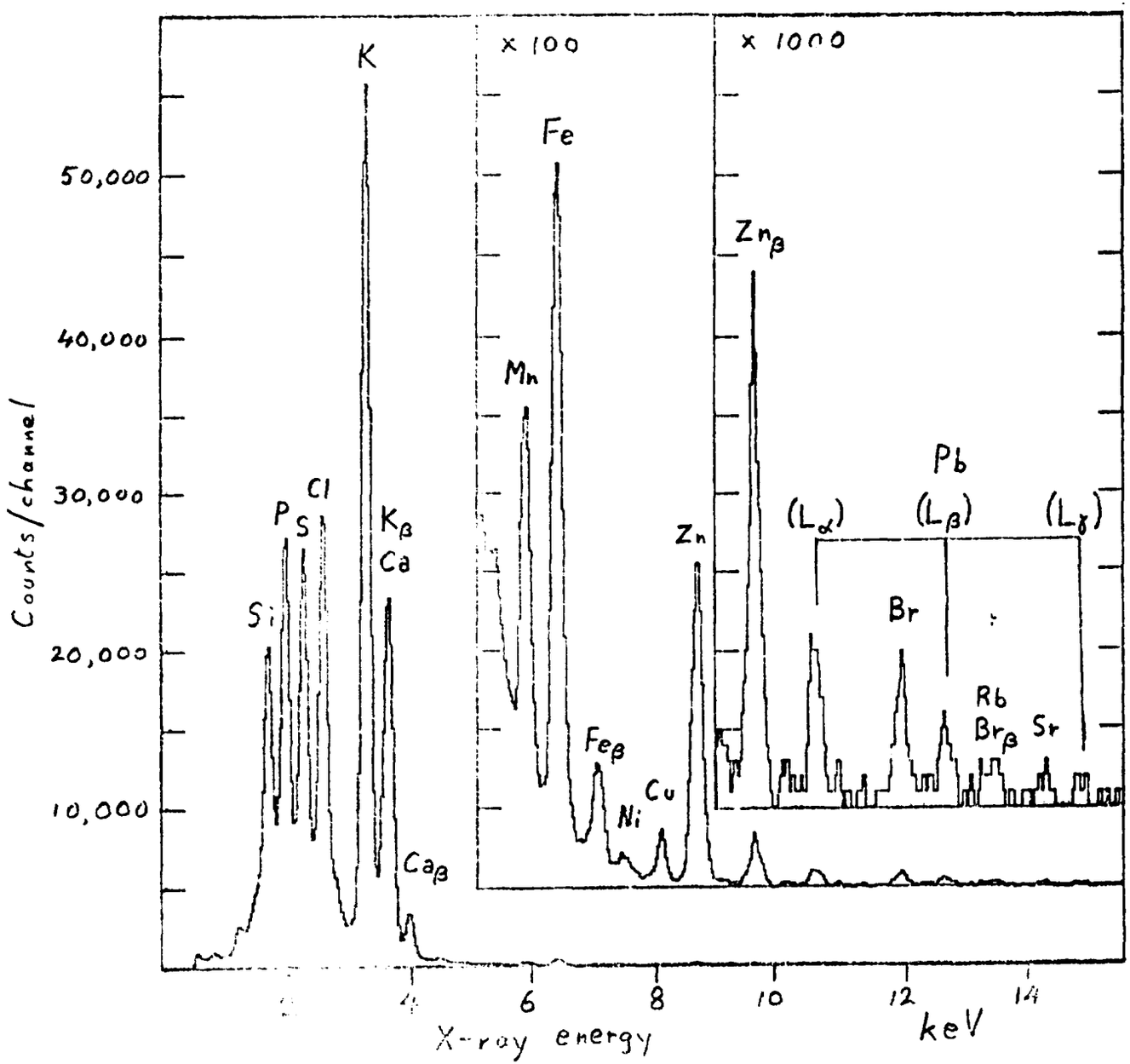
x 100
x 1000
K
Fe
Zn$_\beta$
Mn
Pb
(L$_\alpha$)
(L$_\beta$)
(L$_\gamma$)
Cl
P
S
K$_\beta$
Ca
Si
Zn
Br
Rb
Br$_\beta$
Sr
Fe$_\beta$
Ni
Cu
Ca$_\beta$
50,000
40,000
30,000
20,000
10,000
Counts/channel
4
6
8
10
12
14
X-ray energy
keV

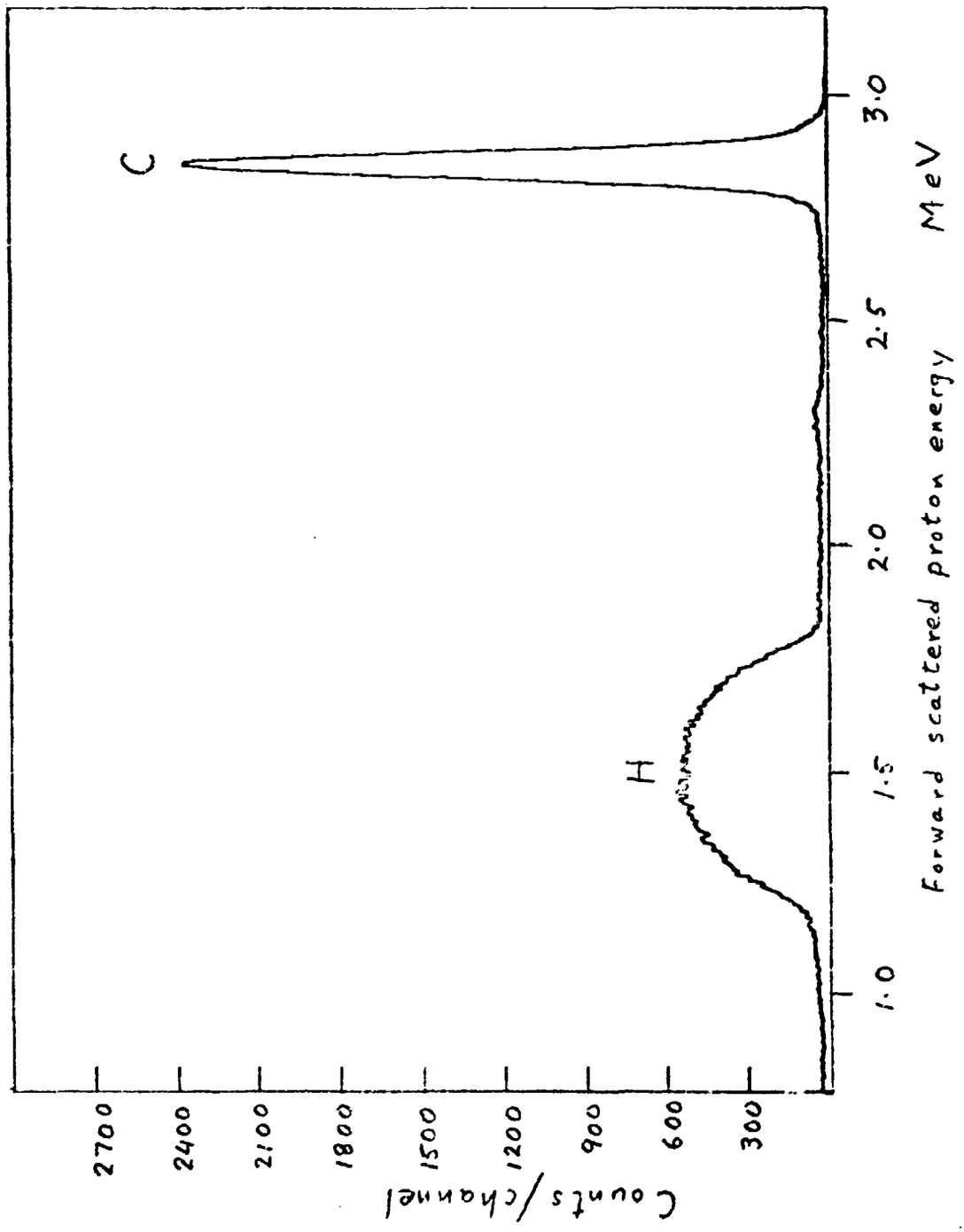
C
H
Counts/channel
2700
2400
2100
1800
1500
1200
900
600
300
1.0
1.5
2.0
2.5
3.0
MeV
Forward scattered proton energy

Figure 6

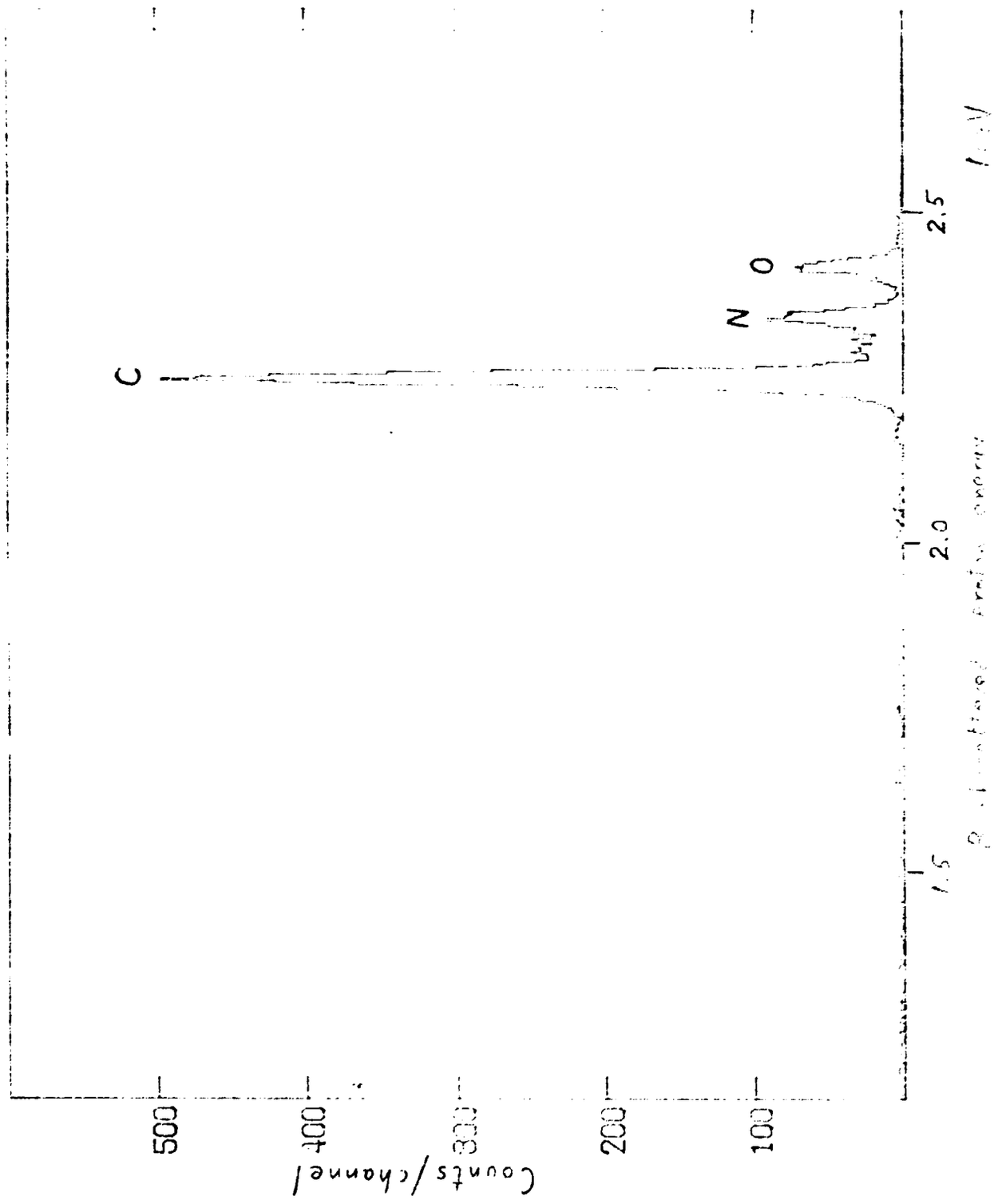

Figure 1

Figure 8

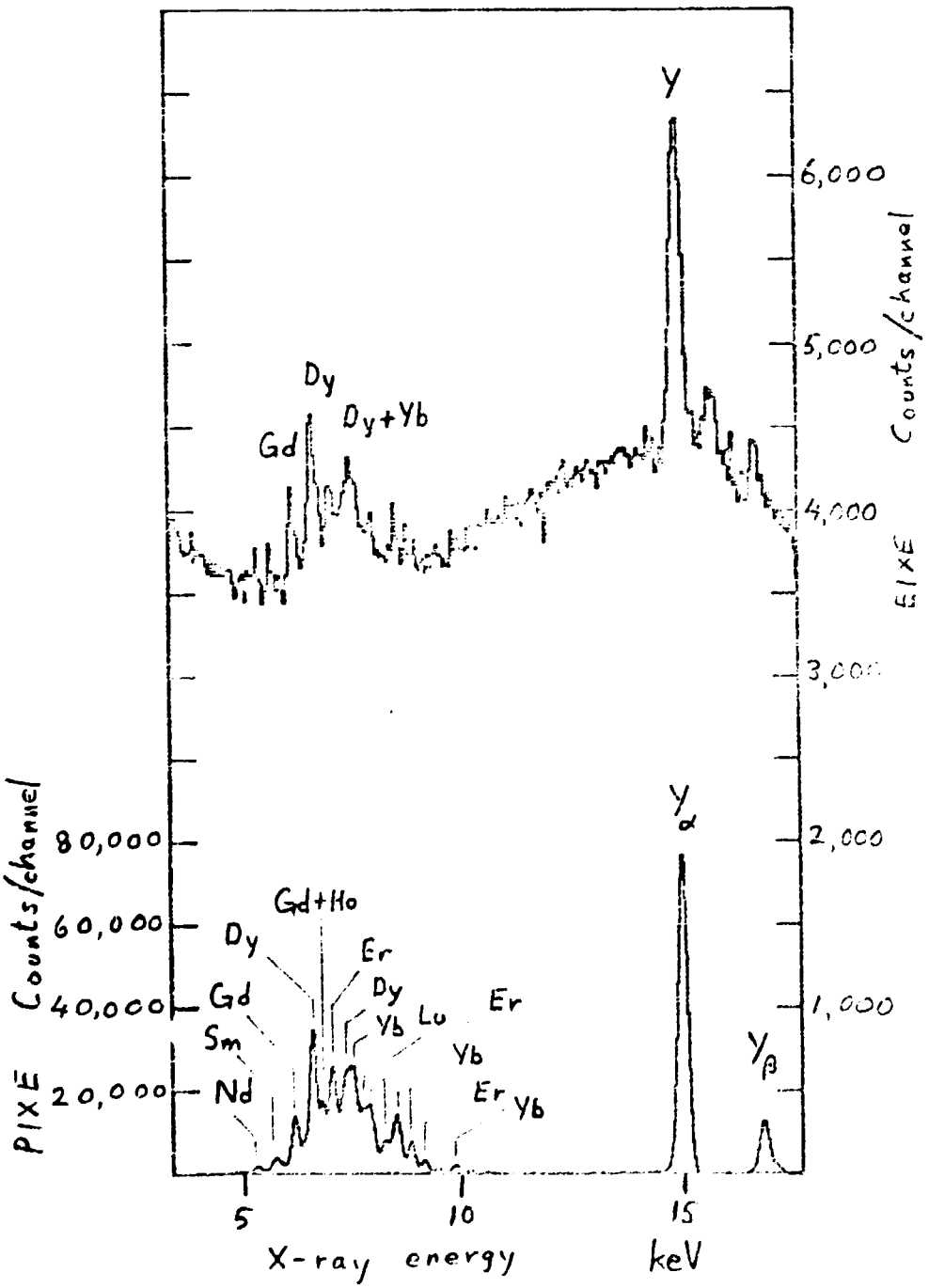
Y
Dy
Dy+Yb
Gd
Gd+Ho
Dy
Er
Dy
Gd
Yb
Lu
Er
Sm
Yb
Nd
Er
Yb
Y_α
Y_β
6,000
5,000
4,000
3,000
2,000
1,000
80,000
60,000
40,000
20,000
PIXE Counts/channel
EIXE Counts/channel
5
10
15
X-ray energy
keV